Resonant High Quality Factor Translucent Lens/Monochromator with Adjustable Focus for Electromagnetic Absorbance Imaging of Micro-Biomolecules

Reza Dehbashi*

Abstract—Characterization of some biological materials relies on absorption imaging. In this paper, a highly translucent flat two-layer structure as part of an imaging system called spectrometer is proposed that has a very high numerical aperture (NA) and high quality factor (QF). The structure can be used to identify micro-biological materials with previously known absorption rate, under single-wavelength electromagnetic absorbance imaging. The proposed two-layer structure is composed of a double-near-zero (DNZ) slab coupled to a high-index dielectric slab with a specific thickness. In DNZ materials, both the permittivity and permeability are close to zero. The DNZ slab operates as a flat lens, and the very high-index dielectric slab functions as a high QF monochromator that at the same time increases NA of the lens without affecting translucidity of the two-layer structure. At the end, a transformation optics (TO) based nonlinear lens is introduced that can be replaced as the DNZ layer. The focus of the nonlinear lens can be tuned by tuning its material parameters.

1. INTRODUCTION

Materials with refractive indices less than one are mostly engineered metamaterials with exotic features which are used in exotic applications like invisibility cloaks [1–3] and flat lenses [4, 5]. Those kinds of materials whose refractive index crosses zero and gets negative values create negative refraction at their interface with non-negative-index materials (i.e., the ordinary material available in the nature). Negative-index materials for the first time were suggested to be used as electromagnetic flat lenses when their refraction index is equal to -1 [5], then it was extended to applications like external cloaking [1]. The negative refraction has been explained for electron waves, as well [6].

Negative-index metamaterials, at the point where the refractive index crosses zero value, can be used for applications like wave-shaping [7] and polarization control [8]. These materials are called zero-index metamaterials. The zero-index materials have been experimentally realized from microwave frequencies [9] to the visible spectrum [10]. A very specific type of zero-index metamaterials is double-near-zero (DNZ) materials which are the focus of this paper. In DNZ materials, both the permittivity and permeability are close to zero [11]. They have recently been used in applications like the size-reduction of electromagnetic devices [12, 13]. In this paper, they are used as part of a proposed lens/monochromator two-layer structure which can be employed for electromagnetic absorbance imaging (EAI). There are some relative works on transmittance coefficient modulation based on meta-materials and metasurfaces [14–16].

In this paper, this EAI as a type of spectroscopy is used to detect and identify the materials with the previously known absorption rate, the parameter which is also called absorbance. Some

micro-biomolecules are detectable by EAI. Three types of them are the focus of this research as they highly interact with wave at some wavelengths of the light. These micro-biomolecules with high absorbance are Deoxyribonucleic (DNA)/ribonucleic (RNA) [17, 18], Tyrosine/Tryptophan [19, 20], and Cytochrome [21–24].

In the proposed two-layer structure, one layer performs as a lens (the DNZ layer), and the other layer (high-index layer) has two roles. One role is to enhance the numerical aperture (NA) of the lens, and the other role is to function as a high quality factor (QF) monochromator to highly reject the wavelengths that interfere with the imaging. The wavelengths for detecting those biomolecules that are targeted in this paper will be specified at the end of this paper.

The index of the DNZ materials is not perfectly equal to zero; therefore, they are not perfect lenses. However, the high index value of the dielectric layer coupled to them can compensate this imperfection. This will be elaborated in Section 4. It is shown that despite using a very high-index value material in the structure, the entire two-layer structure is highly translucent under plane wave illumination. Transparency of the proposed two-layer structure increases intensity of the radiated wave toward the sample under the test without perturbing its performance as a lens/monochromator. In addition, it is proved that the proposed structure has a high QF for the required wavelengths to detect the biomolecules, targeted in this paper. The proposed structure is flat, as well. In the conventional spectrometers, a bulky glass-based or gallium phosphide-based lens with a semi-spherical shape is used to redirect the illuminated wave toward the sample spices [25, 26]. For them, the wave source should be highly aligned at the center of the spherical (or concave and sometimes convex) lens. The source alignment is not required for our proposed flat lens. Obviously, the proposed lens is also less bulky and less heavy than the conventional curved glass made ones. Moreover, for the conventional EAI systems, a separate part is needed as a monochromator to filter out all the unwanted wavelengths while the monochromator is part of the flat lens in our proposed two-layer structure.

At the end, we present a transformation optics (TO) based lens that its directivity can be changed depending on the parameter values of the obtained material. In practice, layers of graphene-based structure can be used, and the material parameters can be tuned by voltage electrodes [27], then like conventional glass-based microscopes, the focus of the light after the flat lens can be changed and tuned.

2. THE IMAGING MECHANISM

For EAI imaging, only a single wavelength is needed to image materials. In this paper, DNZ materials in a two-layer structure are exploited as part of the imaging system. With the advances in the engineered metamaterials, zero-index materials are realizable in practice, particularly, for EAI application where the zero-index feature is only required for a single wavelength. Therefore, any material that both of its constitutive parameters (i.e., permittivity and permeability) are close to zero at just one frequency is suitable for this application. There are materials with zero-index property in the visible spectrum [28]. In the visible spectrum, the micro-biomolecules usually have high absorption in specific frequencies. This characteristic is exploited to identify some biomolecules. With the advances within the last two decades, it is possible to engineer the permittivity or permeability, independently, in a way that both cross the zero value at the same wavelength. For instance, the nano-metallic rods or nano-fishnet structures at nano-scale [29] or simply wires [30] can engineer the permittivity value. Split-ring resonators (SRRs) have been used to engineer permeability [4, 29]. These types of near-zero-index structures can be engineered to be a DNZ material, then can be used in our proposed two-layer lens/monochromator in this paper to image micro-scale biological materials like different types of proteins which will be explained in more details in Section 4.

When a wave passes through a material, it has a reflection and transmission. The reflection and transmission coefficients can be used to identify under illumination materials. Fig. 1 shows these types of imaging. Fig. 1(a) employs the reflection coefficient to identify the unknown material. The reflection-based imaging can be used for medical imaging application, for instance, detecting melanoma in skin cancer. Melanomas have high content of water, which makes them have high permittivity contrast compared to the normal skin. This contrast can be detected by a probe that measures the reflected wave from the skin (Type (a) in Fig. 1(a)). The same applies to some microscopic imaging systems where the amplitude of the reflected signal is measured by a probe, and then, the shape or material
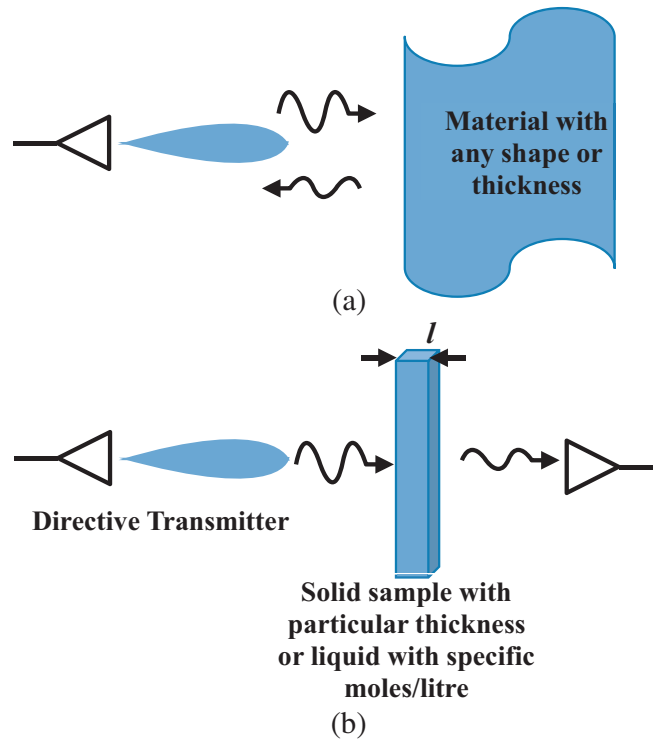
Figure 1. (a) Reflection-based imaging. (b) Absorption-based imaging.

of the surface is obtained. This method relies on a high reflection to detect the imaged object, but for the imaging required for this paper, the reflection level should be as low as possible to obtain high transmission coefficient (the method shown in Fig. 1(b)). Therefore, we propose a two-layer imaging structure that is transparent to the illuminated wave with minimum reflection of the wave for the plane wave illumination. The analytical and numerical analysis to show the transparency of the structure for plane wave illumination will be demonstrated in Section 3.

Figure 1(b) which is the focus of this paper shows an absorbance-based imaging or EAI system which relies on the transmission coefficient of the wave, called absorbance. A directive wave is illuminated to a sample with a specific thickness, and the amplitude of the transmitted wave is measured on the other side of the sample. To obtain a directive illumination, a lens with a high NA is required, and our proposed two-layer structure provides that high NA.

Sometimes the samples are not in solid forms; therefore, they should be dissolved in a liquid. In this case, the moles/litre of the solution must be known. Comparing the measured absorbance with the previously known absorbance for different materials, the sample under the test can be identified. For the liquid form samples, the Lambert-Beer law is applied to identify the sample. For this application, the principal components of an EAI system, called spectrophotometer, are shown in Fig. 2. In Fig. 2, our proposed two-layer structure will be used as the lens/monochromator block. The structure provides high NA by directing a wide angle wave to the test sample. High NA provides high resolution, as well. Therefore, the proposed two-layer structure due to its very high NA can provide very high resolution for some applications in which resolution is very important, as well. However, there is a limit for the resolution provided by the proposed structure. The reason is that to our best knowledge, the highest frequency that a material could have near-zero index feature experimentally is for electromagnetic waves at visible spectrum. Therefore, the proposed two-layer structure cannot be used for applications that work beyond the visible spectrum. For example, the two-layer structure cannot be used for crystallography where the shapes of the biomolecules like proteins are obtained. Proteins are very big molecules; however, they are not big enough to be detected by any lens yet. Their sizes are in the order of 1 nm which is far smaller than the diffraction limit for the visible spectrum, and as discussed before, no near-zero index material has been reported yet in that wavelength. Hence, crystallography,
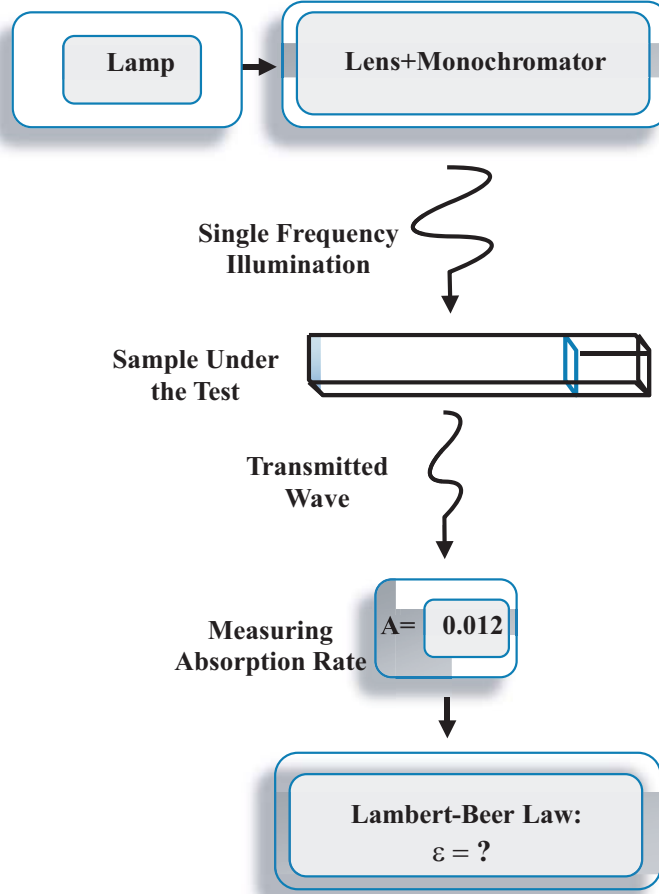
Figure 2. Principal components of a spectrometer to characterize biological species using their absorption rate and Lambert-Beer law [19].

as it is reported in [19], should still rely on X-ray radiation at wavelengths around 0.5 to 3 A° to extract the shape of the biomolecules from the computationally analyzed diffracted rays, or it should use non-lens microscopy techniques like atomic force microscopy (AFM) that a laser beam can detect even 1 A° movement of a nano-size probe moving on the surface of the imaged object. Therefore, the proposed structure cannot image the shape of the biomolecules, and it is only for detecting their type. For that purpose, high NA is required.

High NA for the proposed two-layer structure is due to the DNZ layer where intrinsically provides high NA/resolution. It is also due to the very high index value (n) of the second layer in our proposed two-layer structure. The resolution is conventionally limited by diffraction limit of $0.61\lambda_0$ (λ_0 is the wavelength in the free space), while the proposed structure functions are beyond that limit, as the minimum detectable distance for lenses is proportional to $0.61\lambda_0/n$ [31], where n is the material index. Therefore, by having a high n, high NA is provided, as NA is inversely proportional to the minimum detectable distance (NA $\propto n/0.61\lambda_0$). More details will be explained in Section 4.

3. ANALYSIS OF THE PROPOSED LENS/MONOCHROMATOR UNDER PERPENDICULAR ILLUMINATION (IDEAL SCENARIO)

In this section, behavior of wave for the two-layer structure is analytically and numerically studied when the structure is illuminated by a plain wave, normal to the layers.

3.1. Analytical Analysis

It has been proved that the field inside a DNZ material is uniform [12, 13]. To analytically analyze that, assume that the electric field inside a near zero slab with volume V_d is $\bar{E}_d$ (Fig. 3). Then, the corresponding magnetic field is obtained by:

$$\bar{H}_d = (1/i\omega\mu_0\mu_d)\nabla \times \bar{E}_d \tag{1}$$

In the above equation $\mu_d \approx 0$. Therefore, the electric field $\bar{E}_d$ must be constant inside the entire DNZ slab (volume V_d) to have a finite value for H_d.
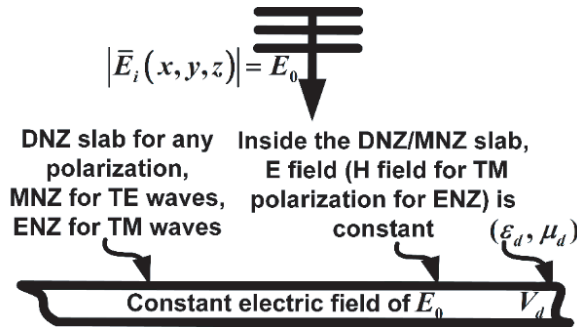
Figure 3. The entire DNZ slab has a constant electric field upon incident of fields with any polarization. For *TE* and *TM* polarized waves, the same happens if the material is MNZ and ENZ, respectively.

Therefore, Maxwell-Ampere law can be applied in a DNZ region when the wave behavior is analyzed. Maxwell's equations and Maxwell-Ampere law are used to derive transmission coefficient of our proposed two-layer structure, shown in Fig. 4.

Assume that a z-polarized (electric field in the Z-direction) plane wave illuminates the structure.
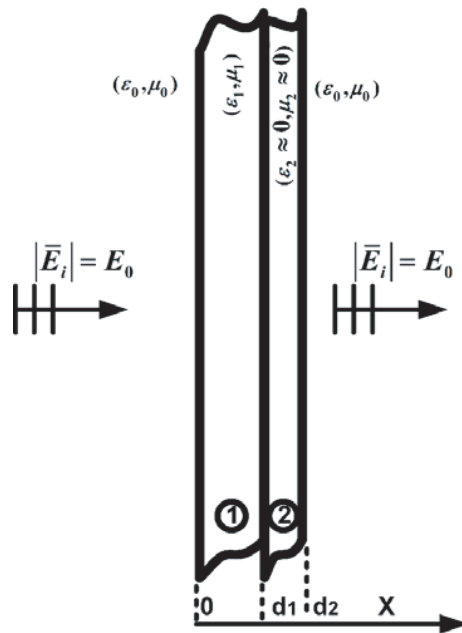
Figure 4. The proposed two-layer structure which consists of a DNZ layer and a high-index dielectric slab. The whole structure is transparent to electromagnetic waves with certain wavelengths under normal incidence.

The fields on the left side are in the following form:

$$x < 0 :$$
$$E_z^l = E_0(e^{-jk0x} + \mathrm{Re}^{jk0x}) \tag{2}$$
$$H_y^l = k_0 E_0(e^{-jk0x} - \mathrm{Re}^{jk0x})/(\omega\mu_0)$$

where k_0 is the wave number in the free space, and R is the reflection coefficient.

In the dielectric region, the fields are:

$$0 < x < d_1 :$$
$$E_z^d = E_0(A_1 e^{-jk1x} + A_2 e^{jk1x}) \tag{3}$$
$$H_y^d = k_1 E_0(A_1 e^{-jk1x} - A_2 e^{jk1x})/(\omega\mu_1)$$

On the other side of the structure, the fields are as:

$$d_2 < x :$$
$$E_z^r = TE_0 e^{-jk0(x-d2)} \tag{4}$$
$$H_y^r = k_0 TE_0 e^{-jk0(x-d2)}/(\omega\mu_0)$$

After applying the boundary conditions and using Maxwell-Ampere law, one can derive the transmission coefficient as:

$$T = 4/((2 - k_0\mu_1/k_1\mu_0 - k_1\mu_0/k_0\mu_1)e^{-jk1d1} + (2 + k_0\mu_1/k_1\mu_0 + k_1\mu_0/k_0\mu_1)e^{jk1d1}) \tag{5}$$

Using the derived equation for T, for the total transmission, the following equation is derived:

$$f_0 = p/(2d\sqrt{\varepsilon_1\mu_1}) \tag{6}$$

where f is the frequency of the incident wave where transparency occurs, and p is an integer number. The parameters ε_1 and μ_1 are the constitutive parameters of layer two (the high-index dielectric layer).

From Eq. (4), for the thickness dielectric of 0.75λ, the entire two-layer structure for dielectric values of 64 and 100 is transparent. Transparency for these values are verified by numerical results and presented in Section 3.2.

3.2. Numerical Analysis

For the proposed two-layer structure, from the previous section's formulations, it is obtained that for dielectric values of 64 and 100, total transmission occurs, while for values of 58.7 and 106, the wave is highly blocked by the structure. These analytical results are vitrified by the simulation results, obtained from a Finite Element (FEM) based electromagnetic (EM) simulator, shown in Figs. 5 and 6. In the simulations, it is assumed that a z-polarized plain wave illuminates the two-layer structure. As illustrated, the wave is not perturbed when the dielectric slab has permittivity values of 64 and 100.

Figure 7 shows the total transmission for two arbitrary thicknesses of DNZ slab when the permittivity value of the dielectric slab is 64. The physical insight for this phenomenon can be explained as follows.

At the beginning of Section 3.1, it is discussed that the fields inside the DNZ slabs are uniform, independent of the thickness of the slab. The simulations also show that the field inside the slab is uniform, and the wave passes across the slab in an instant. The reason is that the phase velocity which is equal to $(\varepsilon_2\mu_2)^{-1/2}$ is close to infinity when ε_1 and μ_1 are close to zero. Therefore, the thickness of the slab does not influence the total transmission effect as the speed of wave is so high that the wave can pass through the slab with any thickness, instantly.

It is noted that for these simulations, loss has been considered very low as near-zero-index materials can have very low loss at their zero-index point. The reason is as follows.

Experimental results show that in wave-matter interaction, there is a point where usually the medium gradually starts to become lossy. It is shown that the point is the beginning of being lossy; therefore, the material has very low loss at that point.

Another study that shows zero-index materials with very low loss is presented in [32]. It shows that a striped pattern of two materials with permittivities equal to 2.65 and 7 can create a near-zero-index
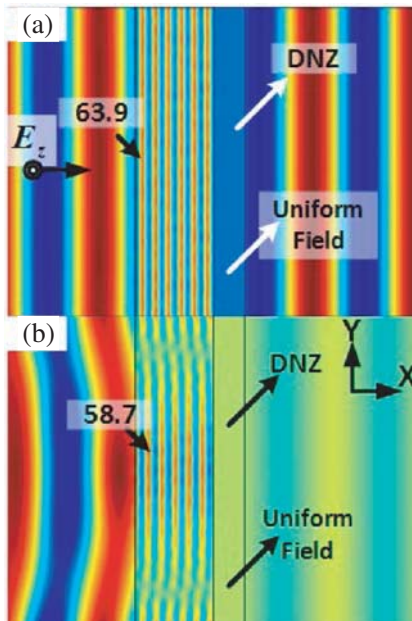
Figure 5. (a) Total transmission for a slab with $\varepsilon_1 = 63.9$ and thickness of $0.75\lambda_0$ beside a DNZ slab with arbitrary thickness. (b) Most of the signal is reflected for $\varepsilon_1 = 58.7$.
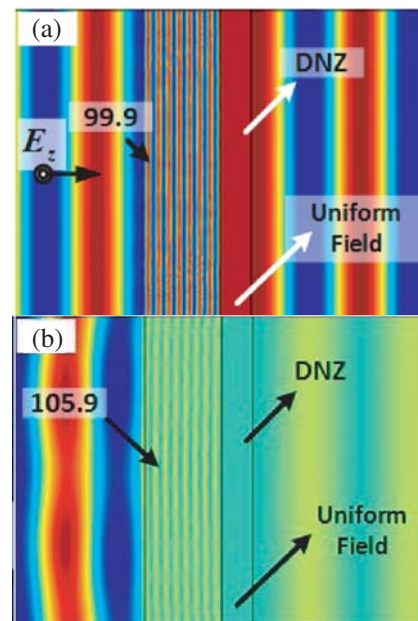
Figure 6. (a) Total transmission for a slab with $\varepsilon_1 = 99.9$ and thickness of $0.75\lambda_0$ near a DNZ slab. (b) Most of the signal is reflected for $\varepsilon_1 = 105.9$.
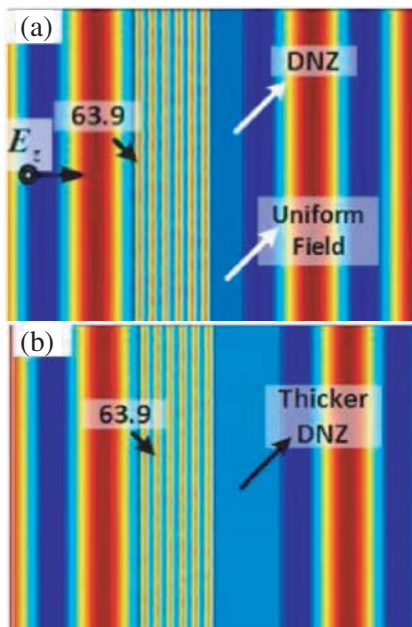
Figure 7. Total transmission through the proposed two-layer structure for two different arbitrary thicknesses of DNZ slab.

structure at a specific wavelength. At the point where the permittivity crosses the zero value, the loss is very low (almost zero).

The next section explains the detection of three types of micro-biomolecule proteins using the proposed two-layer monochromator lens, since they highly interact with wave at three specific wavelengths.

4. DETECTION OF THREE TYPES OF MICRO-BIOMOLECULES

The proposed two-layer structure, as the lens/monochromator part of spectrometers is shown in Fig. 8. As shown, a lamp illuminates light which potentially has a broad spectrum from f_L to f_H. However, for the application targeted by this paper, only one frequency is required as the desired frequency (f_D). The proposed lens/monochromator filters out all the undesired wavelengths and keeps f_D. The layer that contributes to the filtering as the monochromator is the high-index slab layer in which its thickness from Eq. (6) is determined by:

$$d = p\lambda_0/\sqrt{\varepsilon_r} \tag{7}$$

where p is an integer value, λ_0 the desired wavelength at free space, and ε_r the dielectric constant of the monochromator. It will be shown that the monochromator has sufficient QF to distinguish the required wavelength, needed to detect biomolecules listed in Table 1. To our best knowledge, the listed biomolecules in the table are the only ones that can be detected by their absorbance rate, because they highly interact with electromagnetic waves in the visible spectrum range [16].

Table 1. The required thickness for a monochromator for different biomolecule types ($\varepsilon_{r1} = 64$).

Biomolecule type	Nucleotides, e.g., DNA/RNA [14, 15]	Tyrosine/Tryptophan [16, 17]	Cytochrome [18–20]
Absorption wavelength (nm)	260	280	400
Required thickness for monochromator, obtained from Eq. (7) (unit: nm)	16.25, 32.5, . . .	17.5, 35, . . .	25, 50, . . .

As shown in Fig. 8, the monochromatic light is redirected by the two-layer structure to the sample in cuvette with a path length l. A portion of the light absorbed by the sample is then measured and known as absorbance (A). Absorbance parameter A is calculated from the intensity of the illuminating monochromatic wave (I) and the intensity of transmitted wave, passed through the sample cuvette (I):

$$A = \log(I_0/I) \tag{8}$$

Then, Lambert-Beer law is used to calculate extinction coefficient (ε) from the measured absorbance parameter (Fig. 2):

$$\varepsilon = cl/A \tag{9}$$

where c is the moles/liter of the material, dissolved in a liquid. The extinction coefficient obtained by the absorption rate can be used to detect the biomolecules with previously known extinction coefficient. Therefore, by measuring the parameter A and then ε, one can detect and identify the type of some biomolecule species.

All the micro-biomolecules, listed in Table 1, are the examples that can be detected by the proposed two-later structure with the specifications provided in the table for the two-layer structure. To our best knowledge, these are the main proteins that have high absorbance in the visible range.

As mentioned before, in the structure, DNZ layer operates as a lens. The other layer with high-index dielectric value is required as the complementary medium to the DNZ layer to increase its NA. This layer also has an independent role which is a monochromator. The dielectric layer by redirecting the inclined waves to the desired direction which is close to the normal axis of the lens's surface interface increases the NA. For ideal DNZ slabs (where n equals zero), the outgoing wave is always normal to the interface, independent of the direction of incident wave; however, due to non-zero values of permittivity and permeability of non-ideal DNZ slabs, the wave is deviated from the normal axis at the interface. A high-index slab after the lens can correct this deviation and redirect the wave close to the normal axis. It has been illustrated in Figs. 7 and 8. The phenomenon can be explained from the Snell's law of diffraction, as well:

$$n_1 \cdot \sin(\theta_1) = n_2 \cdot \sin(\theta_2) \tag{10}$$
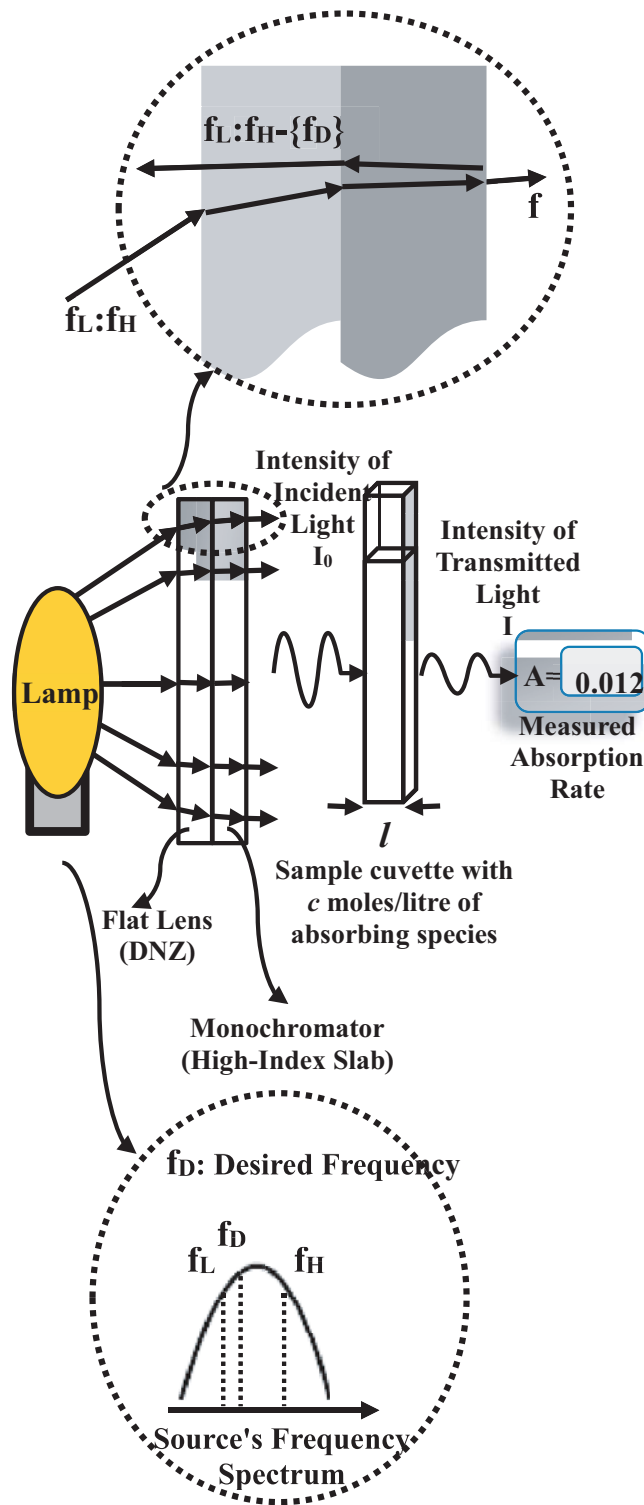
Figure 8. The proposed flat lens/monochromator, illuminated by a lamp. The frequency spectrum of the source is within f_L to f_H. The desired frequency is f_D.

where n_1 and n_2 are the refractive indices of DNZ and high-index dielectric slabs, respectively. The angles are depicted in Fig. 10. If n_1 was zero, the angle θ_2 would have been zero, too, which means that for a perfect zero-index slab, the wave on the right side is normal to the interface, regardless of the
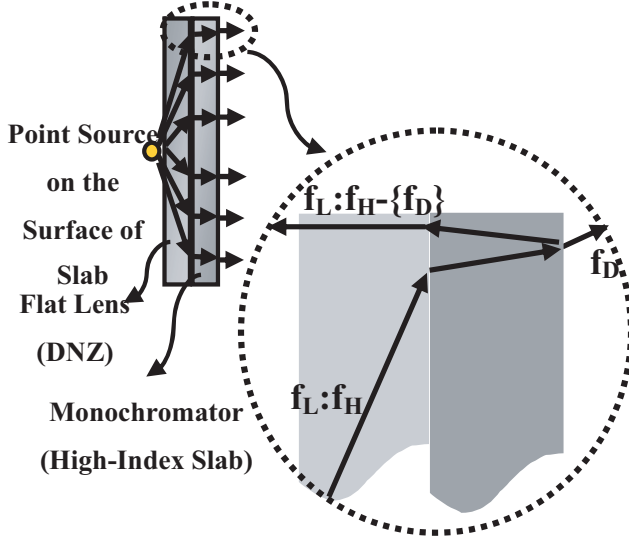
Figure 9. The proposed flat lens/monochromator, illuminated by a point source, located on the surface of DNZ layer.
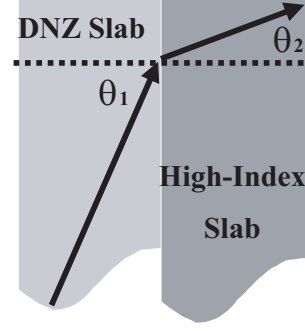
Figure 10. The DNZ/High-index slab interface under oblique illumination.

material of the right side (n_2). However, for a DNZ slab, n_1 is not exactly equal to zero. Therefore, if θ_1 is high, due to an oblique incidence, to achieve a close to zero value for θ_2, n_2 should be high. For instance, if $n_1 = 0.1$ and $\sin(\theta_1) = 0.9$ ($\theta_1 = 65$ degrees), and the other side is free space ($n_2 = 1$), then from Eq. (10), the outgoing wave is inclined with angle $\theta_2 = 5°$. By replacing the free air with a high-index material with $n_2 = 8$ on the right side of the DNZ lens, θ_2 equals $0.6°$ which is almost normal to the interface (highly directive wave). The two-layer structure can even work for point sources like light emission diodes (LED), as the two-layer structure can redirect highly oblique rays, as well, as it is concluded from Eq. (10) and explained in the above example and also illustrated in Fig. 9.

Another benefit of using high-index material as the monochromator is that, from Eq. (7), it reduces the thickness of the required monochromator. However, there is a limit for the value of refractive index of the monochromator. For very high values, the monochromatic performance of the layer becomes very sensitive to small variation of the thickness of the dielectric slab, caused by manufacturing errors. Therefore, ultra high-index materials are not suitable for the monochromator. Despite that, theoretically, very high value of dielectric index can incredibly increase the NA of the DNZ lens and at the same time highly reduce the thickness. An example of a high dielectric value material with almost zero loss in the nature is distilled water with dielectric constant of 81.

Another benefit of DNZ slab as the lens is that the total reflection on its interface never occurs. The condition of total reflection which is also known as critical angle for free-air/DNZ slab is obtained by equating reflection coefficient equal to unity:

$$|\cos(\theta c) - 1|/|\cos(\theta c) + 1| = 1 \tag{11}$$

where θ_c is the critical angle. From Eq. (11), it is obtained that $\theta_c = 90°$. Therefore, for the angles between 0 and $90°$, the total reflection never occurs which means that there is no critical angle for the interface. The critical angle equation, presented in [30], also verifies the above conclusion when intrinsic impedances for interface of two materials are considered equal and when the transmission angle to the second interface is considered as $90°$.

As an example application of the two-layer structure, Table 1 shows the biomolecules that can be detected with the specified thickness for the high-index layer with specifications obtained from Eq. (7). Thickness of the DNZ layer is not important, as it is shown in simulation results in Fig. 7, since it has no effect on the performance of the two-layer structure. It is noted that for the materials listed in Table 1, the molar extinction coefficient (ε) is already known. That is why the biomolecules listed in the table can be identified by EAI, as explained earlier. For instance, at 260 nm, ε of a common micro-biomolecule known as nucleotide is as [14, 15]: $\varepsilon_{260} = 15,400$.

Constituents of Deoxyribonucleic (DNA) and ribonucleic (RNA) as nucleotides, named at Table 1, can be detected as they highly interact with the wave of wavelength 260 nm with previously known extinction coefficient. These nucleotides contain genetic information. The EAI system of Fig. 8 can also be used to detect proteins, as most proteins have high absorbance at 280 nm wavelength. For instance, two aromatic amino acids, tyrosine and tryptophan have absorbance values of 6 and 1.5 at 280 nm at PH6, respectively [16, 17]. Cytochromes are another type of micro-biomolecules with strong absorption at 400 nm, due to the high iron content in their structure [18–20].

As listed in Table 1, the closest required wavelengths for micro-biomolecule detection are 260 and 280 nm. They are fraction of 0.93 of each other. Fig. 11 shows transmission coefficient of the proposed two-layer, obtained from Eq. (5), when the refraction-index of the second layer is 8. As it is shown, if the desired wavelength for the monochromator is 280 nm, and the parameter $|T|$ drops 25% for the next required wavelength, i.e., 260 nm. Therefore, the monochromator has sufficient QF to distinguish the wavelengths required for identifying/detecting biomolecules listed in Table 1. It is again noted that based on our research and best knowledge, the biomolecules listed in Table 1 are the main biomolecules that can be detected, using EAI. Therefore, the wavelengths mentioned in the table are the only wavelengths that can interact with biomolecules and therefore can be used for our proposed EAI system.
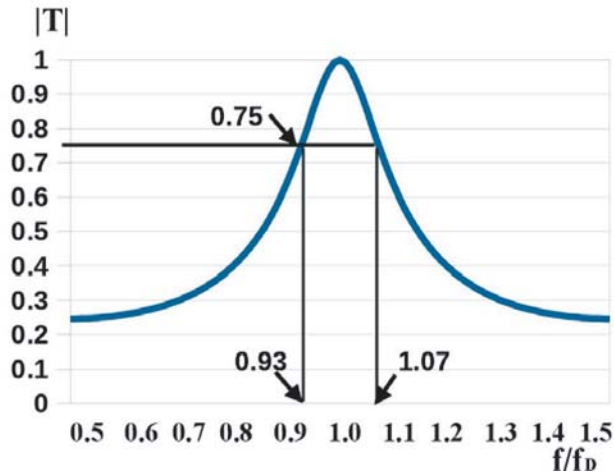
Figure 11. Transmission coefficient vs. frequency for the two-layer structure with $\varepsilon_1 = 64$ and dielectric thickness of $d_1 = 0.75\lambda$ (λ is the wavelength in free space).

It is noted that, in practice, if the working frequency of the DNZ is not matched with the obtained frequency of Eq. (6) and deviates from that, the two-layer structure cannot function very well.

5. NON-LINEAR TRANSFORMATION OPTICS BASED LENS WITH HIGHLY ADJUSTABLE DIRECTIVITY

TO is a technique of producing materials that can manipulate electromagnetic waves in a desired way [1, 3, 5]. Initially the technique was used to design invisibility cloaks [5]. In this section, we introduce a TO-based nonlinear lens whose directivity can be tuned. This lens can be used as the DNZ layer in the previously proposed two-layer structure. If the parameters of the proposed nonlinear lens are tuned, then like conventional glass-based microscopes, the focus of the light after the flat lens can be changed and tuned. In practice, the constitutive parameters of materials like graphene can be tuned by using voltage electrodes and then by tuning the values of the voltage electrodes [31]. Such materials can be employed for the proposed nonlinear lens.

To generate the nonlinear lens using TO, mapping functions are needed. The proposed mappings are shown in Fig. 12 which are as follows:

$$0 \to 0 \tag{12a}$$
$$d_1 \to d_2 \text{ (when } d_2 \to 0) \tag{12b}$$
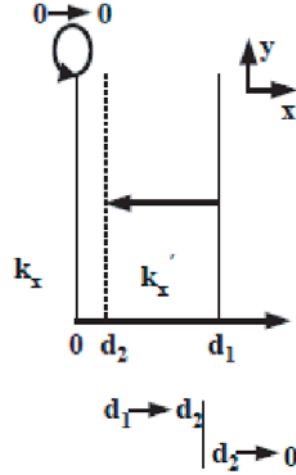
Figure 12. The mappings to obtain material parameters of the proposed non-linear lens with adjustable directivity using transformation optics.

The reason for choosing the transformation mappings in Eq. (12) is that in an ideal case, the slab is a linear zero-index material. For this case, wave instantly travels from one side of the slab to the other side. Therefore, it is like that the wave is mapped from one side to the other side $(d_1 \rightarrow d_2)$. In addition, the transformed space must be matched with the outside material. For that reason, the mapping of (11a) is applied [1, 3]. Moreover, the parameter $d_2 \rightarrow 0$ makes the wavenumber zero, which is essential to creating a near-zero slab in the linear case. The following transformation function can implement the above mappings:

$$f(x') = (d_2^n/d_1^m) x'^m$$
$$d_2 \rightarrow 0 \tag{13}$$
$$n > m, \quad m = 1, 2, 3$$
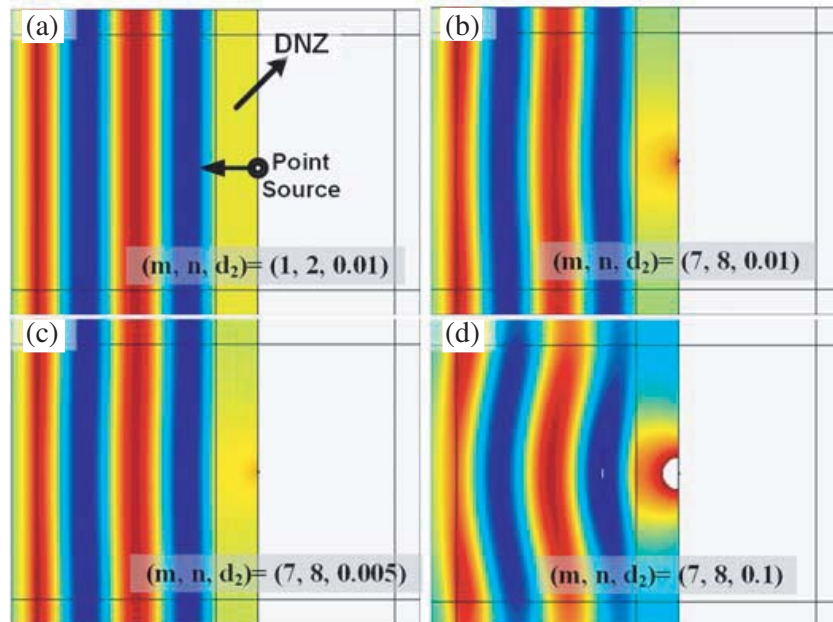
Figure 13. The non-linear lens with different values for parameters of (m, n, d_2) under illumination with a point source adjacent to the lens.

For $m = n = 1$, the lens is a linear type (DNZ material). After applying the function in Eq. (12) to the wave equation when illuminating source is a z-polarized transverse magnetic (TM_z) plane wave and from the TO theory, the material parameters of the transformed space is derived as:

$$\varepsilon_x = \mu_z = \frac{d_2^{n/m}}{\sqrt{d_1\left(\frac{n}{m}\right)\left(\frac{n}{m} - 1\right)}} x^{1-\frac{n}{2m}}$$

$$d_2 \to 0$$

$$n > m, \; m = 1, 2, 3$$

(14)

Figure 13 shows the function of the produced material with different parameters. As it is shown, the wave front has different directivities for different parameter values of the proposed nonlinear lens.

6. CONCLUSION

In this paper, a flat two-layer structure is introduced that can be used in electromagnetic absorbance imaging to detect and identify micro-biomolecules with previously known absorbance. The structure functions as a lens and as a monochromator at the same time. As a flat lens, it has a very high numerical aperture. As a monochromator, it functions as a high quality factor bandpass filter that only allows the desired wavelength to be passed. Finally, a nonlinear lens is introduced which can be replaced as the lens layer. The directivity of the nonlinear lens can be adjusted by tuning its material parameters. Analytical and numerical results about the performance of the proposed structure are in good agreement.

ACKNOWLEDGMENT

REFERENCES

1. Dehbashi, R. and M. Shahabadi, "External cylindrical invisibility cloaks with small material dynamic range," *IEEE Trans. Antenn. Propag.*, Vol. 62, No. 4, 2187, 2014.
2. Dehbashi, R., K. S. Bialkowski, and A. M. Abbosh, 'Uniqueness theorem and uniqueness of inverse problems for lossy anisotropic inhomogeneous structures with diagonal material tensors," *J. Appl. Phys.*, Vol. 121, No. 20, 203103, 2017.
3. Dehbashi, R. and M. Shahabadi, "Possibility of perfect concealment by lossy conventional and lossy metamaterial cylindrical invisibility cloaks," *J. Appl. Phys.*, Vol. 114, No. 24, 244501, 2013.
4. Pendry, J. B., "Negative refraction makes a perfect lens," *Phys. Rev. Lett.*, Vol. 18, No. 85, 3966, 2000.
5. Smith, D. R., J. B. Pendry, and M. C. K. Wiltsgire, "Metamaterials and negative refractive index," *Science*, Vol. 305, 788, 2004.
6. Dehbashi, R., D. Fathi, S. Mohajerzadeh, and B. Forouzandeh, "Equivalent left-handed/right-handed metamaterial's circuit for the massless dirac fermions with negative refraction," *IEEE J. Sel. Top. Quantum Electron.*, Vol. 16, No. 2, 394, 2010.
7. Alu, A., M. G. Silveirinha, A. Salandrino, and N. Engheta, "Epsilon-near-zero metamaterials and electromagnetic sources: Tailoring the radiation phase pattern," *Phys. Rev. B*, Vol. 75, No. 15, 155410, 2007.
8. Alekseyev, L. V., E. E. Narimanov, T. Tumkur, H. Li, Y. A. Barnakov, and M. A. Noginov, "Uniaxial epsilon-near-zero metamaterial for angular filtering and polarization control," *Appl. Phys. Lett.*, Vol. 13, No. 97, 131107, 2010.

9. Liu, R., Q. Cheng, T. Hand, J. J. Mock, T. J. Cui, S. A. Cummer, and D. R. Smith, "Experimental demonstration of electromagnetic tunnelling through an epsilon-near-aero metamaterial at microwave frequencies," *Phys. Rev. Lett.*, Vol. 2, No. 100, 023903, 2008.

10. Mass, R., J. Parsons, N. Engheta, and A. Polman, "Experimental realization of an epsilon-near-zero metamaterial at visible wavelength," *Nat. Photonics*, Vol. 7, 907, 2013.

11. Ahmed, M. M. and N. Engheta, "Wave-matter interactions in epsilon-and-mu-near-zero structures," *Nat. Commun.*, Vol. 5, 5638, 2014.

12. Dehbashi, R., K. S. Bialkowski, and A. M. Abbosh, "Half-sized cylindrical invisibility cloaks using double near zero slabs with realistic material size and properties," *Opt. Express*, Vol. 25, No. 20, 24486, 2017.

13. Dehbashi, R., K. S. Bialkowski, and A. M. Abbosh, "Size reduction of electromagnetic devices using double near zero materials," *IEEE Trans. Antenn. Propag.*, Vol. 65, No. 12, 7102, 2017.

14. Yuan, Y., K. Zhang, B. Ratni, et al., "Independent phase modulation for quadruplex polarization channels enabled by chirality-assisted geometric-phase metasurfaces," *Nat. Commun.*, Vol. 11, 4186, 2020.

15. Yuan, Y., S. Sun, Y. Chen, K. Zhang, X. Ding, B. Ratni, Q. W. Shah, N. Burokur, and C.-W. Qiu, "A fully phase-modulated metasurface as an energy-controllable circular polarization router," *Advanced Science*, Vol. 7, 18, 2020.

16. Zhang, K., Y. Yuan, X. Ding, B. Ratni, S. N. Burokur, and Q. Wu, *ACS Applied Materials & Interfaces*, Vol. 11, No. 31, 28423–28430, 2019.

17. Chang, K. Y. and G. Varani, "Nucleic acids structure and recognitions," *Nat. Struct. Biol.*, Vol. 4 (suppl.), 854, 1997.

18. Friedberg, E. C., G. C. Walker, and W. Siede, *DNA Repair and Mutagenesis*, W. H. Freeman and Company, New York, 1995.

19. Nelson, D. L. and M. M. Cox, *Lehninger Principles of Biochemistry*, W. H. Freeman and Company, 2005.

20. Scopes, R. K., *Protein Purification: Principles and Practice*, 3rd edition, Spring-Verlag, New York, 1994.

21. Crofts, A. R. and E. A. Berry, "Structure and function of the cytochrome bc_1 complex of mitochondria and photosynthetic bacteria," *Curr. Opin. Struct. Biol.*, Vol. 8, 501, 1998.

22. Michel, H., J. Behr, A. Harrenga, and A. Kannt, "Cytochrome c oxidase: Structure and spectroscopy," *Annu. Rev. Biophys. Biomol. Struct.*, Vol. 27, 329, 1998.

23. Tsukihara, T., et al., "The whole structure of the 13-subunit oxidized cytochrome c oxidase at $2.8\,A°$," *Science*, Vol. 272, 113, 1996.

24. Butt, W. D. and D. Keilin, "Absorption spectra and some other properties of cytochrome c and of its compounds with ligands," *Proc. R. Soc. Lond. B Biol. Sci.*, Vol. 156. 429–458, 1962.

25. Mansfield, S. M. and G. S. Kino, "Solid immersion microscope," *Appl. Phys. Lett.*, Vol. 57, No. 24, 2615, 1990.

26. Wu, Q., G. D. Feke, R. D. Grober, and L. P. Ghislain, "Realization of numerical aperture 2.0 using a gallium phosphide solid immersion lens," *Appl. Phys. Lett.*, Vol. 75, No. 26, 4062, 1999.

27. Zhang, Y. and W.-H. Zhu, "Electrically tunable optical devices basedon graphene-split-ring-resonator periodic multilayers at mid-infrared frequencies," *J. Appl. Phys.*, Vol. 128, 133106, 2020.

28. Palik, E. D., *Handbook of Optical Constants of Solids*, Academic, 1998.

29. Cai, W. and V. Shalaev, *Optical Metamaterials: Fundamentals and Applications*, Springer, 2009.

30. La Spada, L. and L. Vegni, "Near-zero-index wires," *Opt. Express*, Vol. 25, No. 20, 23699, 2017.

31. Balanis, C. A., *Advanced Electromagnetic Engineering*, 2nd edition, John Wiley & Sons, New York, 2012.

32. Isakov, D. V., et al., "3D printed anisotropic dielectric composite with meta-material features," *Mater. Des.*, Vol. 93, 423, 2016.